RESEARCH ARTICLE

WILEY

Frequency-dependent modulation of neural oscillations across the gait cycle

Mingqi Zhao[1] | Gaia Bonassi[2] | Jessica Samogin[1] |
Gaia Amaranta Taberna[1] | Elisa Pelosin[3,4] | Alice Nieuwboer[5] |
Laura Avanzino[4,6] | Dante Mantini[1]

[1]Movement Control and Neuroplasticity Research Group, KU Leuven, Leuven, Belgium

[2]S.C. Medicina Fisica e Riabilitazione Ospedaliera, Chiavari, Italy

[3]Department of Neuroscience, Rehabilitation, Ophthalmology, Genetics and Maternal Child Health, University of Genova, Genova, Italy

[4]IRCCS Ospedale Policlinico San Martino, Genoa, Italy

[5]Department of Rehabilitation Sciences, KU Leuven, Leuven, Belgium

[6]Department of Experimental Medicine, Section of Human Physiology, University of Genoa, Genoa, Italy

Correspondence
Dante Mantini, Movement Control and Neuroplasticity Research Group, KU Leuven, Tervuursevest 101, Leuven 3001, Belgium.
Email: dante.mantini@kuleuven.be

Abstract

Balance and walking are fundamental to support common daily activities. Relatively accurate characterizations of normal and impaired gait features were attained at the kinematic and muscular levels. Conversely, the neural processes underlying gait dynamics still need to be elucidated. To shed light on gait-related modulations of neural activity, we collected high-density electroencephalography (hdEEG) signals and ankle acceleration data in young healthy participants during treadmill walking. We used the ankle acceleration data to segment each gait cycle in four phases: initial double support, right leg swing, final double support, left leg swing. Then, we processed hdEEG signals to extract neural oscillations in alpha, beta, and gamma bands, and examined event-related desynchronization/synchronization (ERD/ERS) across gait phases. Our results showed that ERD/ERS modulations for alpha, beta, and gamma bands were strongest in the primary sensorimotor cortex (M1), but were also found in premotor cortex, thalamus and cerebellum. We observed a modulation of neural oscillations across gait phases in M1 and cerebellum, and an interaction between frequency band and gait phase in premotor cortex and thalamus. Furthermore, an ERD/ERS lateralization effect was present in M1 for the alpha and beta bands, and in the cerebellum for the beta and gamma bands. Overall, our findings demonstrate that an electrophysiological source imaging approach based on hdEEG can be used to investigate dynamic neural processes of gait control. Future work on the development of mobile hdEEG-based brain–body imaging platforms may enable overground walking investigations, with potential applications in the study of gait disorders.

KEYWORDS
Electroencephalography (EEG), gait analysis, mobile brain–body imaging (MoBI), motor control, neural activity

---

1 | INTRODUCTION

Walking is a common activity of daily living and at the same time a very complex one. Normal gait requires a delicate balance between various interacting neuronal systems and consists of three primary components: balance, or standing stability; locomotion, including initiation and maintenance of rhythmic stepping; and the ability to adapt to the environment (Hamacher et al., 2015). Gait impairments may strongly restrict the personal independence and affect the quality of life (Baker, 2018). Gait and balance problems may be precursors of falls, the most common cause of injuries in the elderly (Alexander, 1996; Sudarsky, 1990). Furthermore, walking is an important indicator of the overall health status. For instance, it has been shown that the self-selected walking speed correlates with individual life expectancy in the elderly population (Studenski et al., 2011).

Normal gait has been extensively characterized from a biomechanical perspective, leading to the identification of several consecutive phases that occur cyclically (Alamdari & Krovi, 2017; Schmeltzpfenning & Brauner, 2013; Silva & Stergiou, 2020). First of all, initiating gait requires a stable upright body position. To start walking, one leg is raised and directed forward by flexing the hips and knee. The normal forward step consists of two phases: stance phase and swing phase. The stance phase occupies 60% of the gait cycle, during which one leg and foot are bearing most or all of the bodyweight. The swing phase occupies only 40% of it, during which the foot is not touching the walking surface and the bodyweight is supported by the other leg and foot. In a complete two-step cycle, both feet are simultaneously in contact with the floor for about 25% of the time. This part of the cycle is called the double-support phase, to distinguish it from the single-support phase.

At the neural level, gait is orchestrated through the activity of neural assemblies in cortical and subcortical regions (Bakker, Verstappen, et al., 2007; Takakusaki, 2017). Those brain regions dynamically exchange information with each other, and send/sense neural pulses through the spinal cord to/from the body parts in order to control the gait process (Takakusaki, 2017). The role of different brain regions in supporting gait, however, remains insufficiently understood. For instance, positron emission tomography (PET), functional magnetic resonance imaging (fMRI), and single photon emission computer tomography (SPECT) studies documented the activation of the primary sensorimotor cortices (S1/M1), the supplementary motor area (SMA), the thalamus, and the cerebellum following actual walking (Fukuyama et al., 1997), as well as during stereotypical lower limb movements (Sahyoun et al., 2004) and pedaling (Christensen et al., 2000). In addition, the activation of S1/M1 and SMA has also been observed during imaginary walk (Jahn et al., 2004; Sacco et al., 2006). PET, fMRI, and SPECT are not well suited, however, for the study of brain dynamics during actual walking, which may be key for a better understanding of mechanisms of gait control (Bakker, Verstappen, et al., 2007). Functional near-infrared spectroscopy (fNIRS) can be effectively used for the study of brain activity in mobile conditions, including walking conditions. Notably, the results obtained with fNIRS during gait were consistent with those reported in several brain imaging studies (Kurz et al., 2012; Miyai

et al., 2001; Suzuki et al., 2004; Suzuki et al., 2008). However, fNRIS cannot be used to investigate neural dynamics during gait, as the signals it measures are mediated by hemodynamic processes (Ferrari & Quaresima, 2012).

Electroencephalography (EEG) is an alternative technique to study brain activity in mobile conditions. EEG records variations in scalp voltages that are directly produced by neuronal activity in different brain regions. EEG signals display a combination of slow and fast neuronal oscillations. In the frequency domain, these oscillations are typically classified as delta (1–4 Hz), theta (4–8 Hz), alpha (8–13 Hz), beta (13–30 Hz), and gamma (>30 Hz) oscillations (Mantini et al., 2007). The power of neural oscillations was found to be modulated by motor behavior. For instance, alpha and beta power decreases in the contralateral portion of S1/M1 during hand movement, and rebounds when the movement terminates (Pfurtscheller, 2001). Such event-related effect can be explained by the change in excitability of local neurons (Neuper et al., 2006; Stolk et al., 2019), and is often referred to as event-related desynchronization/synchronization (ERD/ERS; Pfurtscheller & Lopes da Silva, 1999).

A number of studies have attempted to investigate gait-related neural dynamics using mobile EEG. Particularly, an ERD/ERS analysis called gait event-related spectral perturbation (GERSP) was frequently applied to examine changes of neural oscillations across the gait cycle (Gwin et al., 2011). For example, a coupling between gait cycle and electrocortical activity over the central sensorimotor cortex was observed during treadmill walking (Gwin et al., 2011). Similar studies identified the suppression of beta-band oscillations during walking (Seeber et al., 2014) and reported a reverse modulation of low and high gamma oscillations in central sensorimotor cortex (Seeber et al., 2015). Notably, a similar modulation pattern was also found with EEG during pedaling (Storzer et al., 2016). Another EEG study suggested the involvement of prefrontal, posterior parietal and sensorimotor regions in controlling the speed of walking (Bulea et al., 2015). A more recent study observed unidirectional brain to muscle connectivity during walking (Artoni et al., 2017). It should be noted that EEG data in almost all studies were analyzed at the sensor rather than at the source level, limiting the interpretability of the findings in relation to the underlying neural generators.

In recent years, novel technical developments have opened the way for the use of EEG as a brain imaging tool (Michel & Murray, 2012). Specifically, the application of high-density electroencephalography (hdEEG) (Liu et al., 2015) in combination with novel realistic head modeling methods (Taberna, Guarnieri, & Mantini, 2019; Taberna, Marino, et al., 2019; Taberna, Samogin, & Mantini, 2021) has permitted more accurate characterization of neural oscillations in the source space. For instance, our group has used hdEEG in previous studies for analyzing the functional dissociation of body movements (Zhao et al., 2019), the topology of resting-state brain networks (Liu et al., 2017; Liu et al., 2018), and the assessment of frequency-dependent connectivity in the human brain (Samogin et al., 2019, 2020). To the best of our knowledge, few studies have used hdEEG to investigate gait-related neural oscillations in the brain, possibly due to the presence of large artifacts in mobile conditions (Castermans

et al., 2014; Nathan & Contreras-Vidal, 2016). Recently, we proposed an artifact attenuation method that proved particularly effective with hdEEG data collected in walking participants (Zhao et al., 2021).

The general goal of this study was to characterize frequency-dependent modulations of neural oscillations in the human brain across the gait cycle. More specifically, we aimed at examining whether the main gait-related neural sources were localized in the primary sensori-motor cortex, and whether the power of neural oscillations was different across frequency bands and gait phases. To this end, we performed hdEEG recordings in a group of healthy participants during treadmill walking. Based on these hdEEG data, we conducted an ERD/ERS analysis in selected regions of interest (ROIs) and then examined ERD/ERS maps across different gait phases in alpha, beta, and gamma bands. First, we verified that the primary neural sources were spatially localized in the primary sensorimotor cortex, and in particular in the portion associated with leg movements (Zhao et al., 2019). Next, we specifically tested the hypothesis that modulations of the alpha-, beta- and gamma-band neural oscillations were dissociable across gait phases. Overall, our study aims to contribute to a better understanding of neural processes underlying gait performance.

2 | METHODS

2.1 | Experiment and data

Twenty-four healthy participants (14 females and 10 males, age 22–31 years) without any brain-related injury/disease or serious medical condition were recruited for the experiment. The experimental procedures were approved by the Ethics Committee of the Liguria Region, Italy (reference: 238/2019) and were conducted in accordance with the 1964 Helsinki declaration and its later amendments. An informed consent was obtained from each participant.

During the experiment, the participant was asked to walk on a Forcelink treadmill (Motek Medical B.V., Houten, the Netherlands) with normal, self-selected speed (Gwin et al., 2011; Wagner et al., 2016). The task design consisted of three blocks of walk, each lasting 2 min, with 1-min rest in-between. During the experiment, we collected 128-channel hdEEG data using an ActiCHamp amplifier (Brain Products GmbH, Gilching, Germany). The hdEEG sensors, integrated in an EEG cap with standard 10/20 montage, were connected to the participant's scalp through a conductive gel. The hdEEG data were sampled at 1 kHz frequency, using the FCz electrode as physical reference. Simultaneously with hdEEG signals, we also collected three-axis acceleration signals from the participant's ankles using a Trigno wireless platform (Delsys Inc., Natick, MA). Acceleration signals were sampled at 148 Hz frequency. The temporal jitter between hdEEG data and acceleration signals was quantified experimentally and resulted in being below 5 ms. Immediately after the experiment, we acquired a 3D scan of the participant's head using an iPad (Apple Inc., USA) equipped with Structure Sensor (Occipital Inc., Boulder, CO) to extract the locations of the hdEEG electrodes (Taberna, Marino, et al., 2019; Taberna, Samogin, & Mantini, 2021).

In a separate session, the structural MR image of each participant's head was collected with a 3 T Philips Achieva MR scanner (Philips Medical Systems, the Netherlands) using a T1-weighted magnetization-prepared rapid-acquisition gradient-echo (MP-RAGE) sequence. The scanning parameters were: repetition time (TR) = 9.6 ms, echo time (TE) = 4.6 ms, 160 coronal slices, 250 × 250 matrix, voxel size = 0.98 × 0.98 × 1.2 mm^3.

2.2 | Behavioral analysis

For each participant, we first calculated the total acceleration of left and right ankle separately, and then integrated them to obtain velocity estimates. Data segments with stable velocity were then isolated and included in further analyses. Acceleration signals were used to detect gait events for each cycle (e.g., see Figure 1), in line with previous studies (Jasiewicz et al., 2006; Kotiadis et al., 2010). These events were: left heel strike (LHS), right heel strike (RHS), left toe off (LTO), and right toe off (RTO) (Gwin et al., 2011; Seeber et al., 2014; Wagner et al., 2016). Based on the detected gait events, we divided each gait cycle into four phases (Figure 1): initial double support (IDS) between LHS and RTO, right leg swing (RLS) between RTO and RHS, final double support (FDS) between RHS and LTO, and left leg swing (LLS) between LTO and LHS (Artoni et al., 2017; Laribi & Zeghloul, 2020). Based on the ankle acceleration signals, the number of gait cycles and the average walking speed were also quantified.
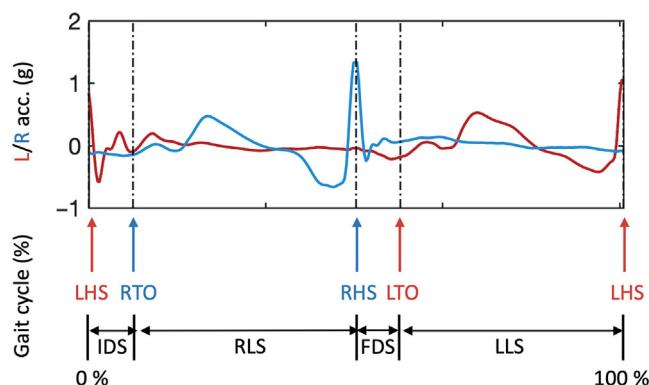
FIGURE 1 Analysis of gait phases based on left (red) and right (blue) ankle acceleration signals. We identified each gait cycle, starting from a LHS event and ended with the next LHS event. Between the two LHS events, we detected RTO, RHS, and LTO events, respectively. The heel strike events (i.e., LHS and RHS) corresponded to a sharp pulse of the ipsilateral acceleration signal, while the toe off events corresponded to the start of the gradual increase of the same signal. These gait events divided a gait cycle in four phases, two of which corresponding to double support states with two legs (i.e., IDS and FDS), and the other two corresponding to single support states with one of the legs swinging off the ground (i.e., RLS and LLS). LHS, left heel strike; RHS, right heel strike; LTO, left toe off; RTO, right toe off; IDS, initial double support; RLS, right leg swing; FDS, final double support; LLS, left leg swing

2.3 | EEG analysis

HdEEG data were analyzed to evaluate dynamic modulations of brain oscillations in walking conditions. The analysis involved three main steps: data preprocessing, head model creation, and ERD/ERS imaging (Liu et al., 2017; Samogin et al., 2019; Samogin et al., 2020; Taberna, Samogin, Marino, & Mantini, 2021; Zhao et al., 2019).

2.3.1 | Data preprocessing

We first corrected the hdEEG data for bad channels (Guarnieri et al., 2018), digitally filtered them in the band [1–80] Hz and down-sampled them to 200 Hz. Then, we applied the multi-step blind source separation (BSS) approach that we presented in one of our recent studies (Zhao et al., 2021) to minimize the impact of ocular, movement and myogenic artifacts that were mixed in the hdEEG signals. Each step in the approach addressed one of the three artifact categories using a specific BSS method and an optimized artifact classification parameter. Specifically, in the first step, we decomposed the data using FastICA-defl (Hyvarinen, 1999), and the components with maximum kurtosis (calculated in a 5-s sliding window) greater than 12 were considered as ocular artifacts. In the second step, we decomposed the data using FastICA-symm (Hyvarinen, 1999), and the components with mean sample entropy (calculated in a 20-s sliding window) lower than 0.8 were considered as movement artifacts. In the last step, we decomposed the data using independent vector analysis (Anderson et al., 2011), and the components with a gamma band (30–80 Hz) to a whole band (1–80 Hz) power ratio higher than 0.5 were classified as myogenic artifacts. Finally after the artifact attenuation, we re-referenced the data to the average reference (Liu et al., 2015).

2.3.2 | Head model creation

The calculation of a leadfield matrix, which relates the activity of each individual brain source to the electrical potentials measured over the scalp, is required for source signal reconstruction. To calculate such a matrix we followed three main processing steps: *Electrodes position detection and coregistration; Head tissue segmentation; and Leadfield matrix calculation* (Taberna, Samogin, Marino, & Mantini, 2021). (1) *Electrodes position detection and co-registration*. The precise locations of the EEG electrodes were first detected using SPOT3D toolbox (Taberna, Guarnieri, & Mantini, 2019; Taberna, Marino, et al., 2019) from the 3D scans, and then co-registered to the scalp of each individual MR image; (2) *Head tissue segmentation*. The individual MR images were segmented into 12 tissue layers (skin, eyes, muscle, fat, spongy bone, compact bone, cortical/subcortical gray matter, cerebellar gray matter, cortical/subcortical white matter, cerebellar white matter, cerebrospinal fluid, and brain stem) using the MR-TIM software (Taberna, Samogin, & Mantini, 2021). The conductivity of each tissue was set according to previous studies (Haueisen et al., 1997; Holdefer et al., 2006); and (3) *Leadfield matrix calculation*. We meshed the tissue layers to 6-mm hexahedrons and positioned source dipoles in the hexahedrons that were inside the gray matter. To calculate the leadfield matrix for each participant, we used the Simbio finite element method integrated in the FieldTrip toolbox (Vorwerk et al., 2018).

2.3.3 | ERD/ERS imaging

We fed the individual head model together with the preprocessed hdEEG data to the exact low-resolution brain electromagnetic tomography (eLORETA) algorithm (Pascual-Marqui et al., 2011), in order to estimate neural signals for each voxel in the gray matter. Based on the estimated neural signals, frequency-dependent modulations of neural oscillations were assessed by conducting an ERD/ERS analysis.

We initially restricted our analysis to six ROIs that were relevant to the gait control processes (Bakker, Verstappen, et al., 2007; Seeber et al., 2015). These ROIs were located at SMA, right M1, left M1, thalamus, right cerebellum, and left cerebellum (see Table 1 for MNI coordinates). For each ROI, the MNI coordinates were transformed into individual space. A representative ROI signal was defined as the first principal component of signals from the voxels within a 6-mm sphere centered on the coordinates in individual space. Then, the spectrogram of the signal, as estimated using a continuous wavelet transformation (CWT, number of octaves = 6, voices per octave = 8), was epoched according to the onset/offset of each gait cycle. After warping the epochs to a common temporal scale (0%–100% of the gait cycle), we averaged them to perform an ERD/ERS analysis (Artoni et al., 2017; Gwin et al., 2011; Seeber et al., 2015). The resulting ERD/ERS map was then averaged in each gait phase, separately for alpha (8–13 Hz), beta (13–30 Hz), and gamma (30–50 Hz) bands. The significance of these ERD/ERS intensities were evaluated using paired t-tests, corrected for multiple comparisons using the false discovery rate (FDR) method. Finally, we used a two-way analysis of variance (ANOVA) for each ROI to test the effect of frequency band and gait phase, as well as their interaction, on ERD/ERS intensity. To further test the presence of lateralized ERD/ERS modulations in bilateral ROIs (i.e., M1 and cerebellum) for each frequency band, we examined the interaction between ROI side and gait phase by means of a two-way ANOVA.

TABLE 1 Montreal Neurological Institute (MNI) coordinates for selected regions of interest (ROIs)

ROI	MNI coordinates
Supplementary motor area (SMA)	[0, −8, 56]
Left primary motor cortex (left M1)	[−34, −12, 68]
Right primary motor cortex (right M1)	[34, −12, 68]
Thalamus	[0, −18, 11]
Left cerebellum	[−27, −80, −38]
Right cerebellum	[27, −80, −38]

Next, we extended the ERD/ERS analysis to brain activity reconstructed in all voxels. Accordingly, we obtained volumetric ERD/ERS images for each frequency band and gait phase. The volumetric images were warped to MNI space, then averaged across participants, according to a fixed-effect group analysis. To examine the main effects and interaction of frequency band and gait phase, we performed a voxel-wise two-way ANOVA on the ERD/ERS images of all the participants. The resulting statistical parametric maps were thresholded at $p < .01$ and corrected for multiple comparisons using the FDR method. We also examined spatial similarities of the group-level ERD/ERS images across frequency bands and gait phases by calculating their spatial correlation.

3 | RESULTS

3.1 | Gait-related neural modulations in ROIs

The analysis of neural signatures in the gait cycle required the detection of gait events and gait cycles, which was performed using the acceleration of the ankles. From about 200 up to more than 400 gait cycles were included for each participant, with average walking speed ranging between 1.9 and 3.1 km/h (Figure 2, Table S1). Then, we extracted ERD/ERS values for different motor-related ROIs (Figure 3), and tested their significance for each frequency band and gait phase (Figure 4). For the alpha and beta bands, we observed ERS in left/right M1, SMA, and thalamus during double support phases (IDS and FDS), and ERD at comparable frequencies during swing phases (LLS and RLS). The beta ERD in the leg swing phases showed significantly stronger intensity in the contralateral M1 than the ipsilateral M1 ($p < 0.001$). For the gamma band, we observed ERS during the leg swing phases and ERD during the double support phases for SMA and thalamus. Specifically, the gamma ERS was more prominent in the thalamus and SMA than in M1 ($p = 0.021$ and 0.034, respectively).

To evaluate the effects of frequency band and gait phase on neural power modulations, we performed a two-way ANOVA for each ROI (Table S2). The results did not show any significant effect of frequency band for the ROIs, whereas significant differences were found

across phases for SMA ($p < .001$), M1 ($p < .001$ for both sides), and the cerebellum ($p = .01$ for the right side, and $p < .001$ for the left side). The analysis also revealed a significant interaction between frequency band and gait phase in SMA, M1, thalamus, and left cerebellum ($p < .001$ for all ROIs). For the leg swing phases (RLS and LLS), we observed stronger beta ERD in contralateral M1 than in ipsilateral M1. We further examined lateralized ERD/ERS patterns across gait phases for the bilateral ROIs, as revealed by the interaction between the ROI side and gait phase using an ANOVA (Table S3). This analysis evidenced lateralized modulations of ERD/ERS in M1 for alpha ($p = .001$) and beta bands ($p = .003$), as well as in the cerebellum for beta ($p = .004$) and gamma bands ($p < .001$).

3.2 | Whole-brain analysis of neural sources during gait

We extended the ERD/ERS analysis to the whole-brain level, by calculating ERD/ERS images across frequency bands and gait phases (Figure 5). We observed alpha- and beta-band ERS for the two double support phases (IDS and FDS), as well as alpha- and beta-band ERD for the two leg swing phases (RLS and LLS), with strong intensity mainly over the sensorimotor cortex, the premotor cortex, and the cerebellum. Specifically, the ERS of IDS appeared more in the left sensorimotor cortex, whereas the ERS of FDS was more prominent in the right sensorimotor cortex. The ERD in the alpha band was more dorsal, whereas it was rather ventral and lateralized in the beta band. In the gamma band, we found an ERS for the two swing phases over the premotor cortex and close to the thalamus.

As a final analysis step, we assessed differences and similarities of the ERD/ERS images across frequency bands and gait phases. We tested differences using a voxel-wise two-way ANOVA with frequency band and phase as factors (Figures 6). According to this analysis, no region had ERS/ERD that was exclusively modulated by the frequency band. Conversely, significant differences were found across gait phases in bilateral sensorimotor cortex and cerebellum. We observed a significant interaction between frequency band and gait phase in the premotor cortex and the thalamus. In addition, the analysis of similarities between ERD/ERS images evidenced a significant positive correlation ($r = 0.47$, $p < .001$) between adjacent frequency bands for the same gait phase (Figure 7a), and a significant negative correlation ($r = -0.29$, $p < .001$) between adjacent gait phases for the same frequency band (Figure 7b).

4 | DISCUSSION

In this study, we aimed at assessing the spatial distribution of active neural sources during gait, and at examining how the power of neural oscillations in the brain was modulated across gait phases. To this end, we quantified frequency-dependent modulations of neural oscillations during walking using hdEEG. In comparison to previous studies, our study has two specific merits: it employed advanced techniques
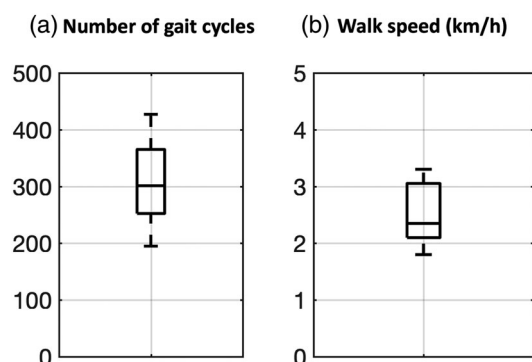

FIGURE 2 Gait performance across participant. (a) Number of gait cycles of each participant. (b) Walking speed of each participant
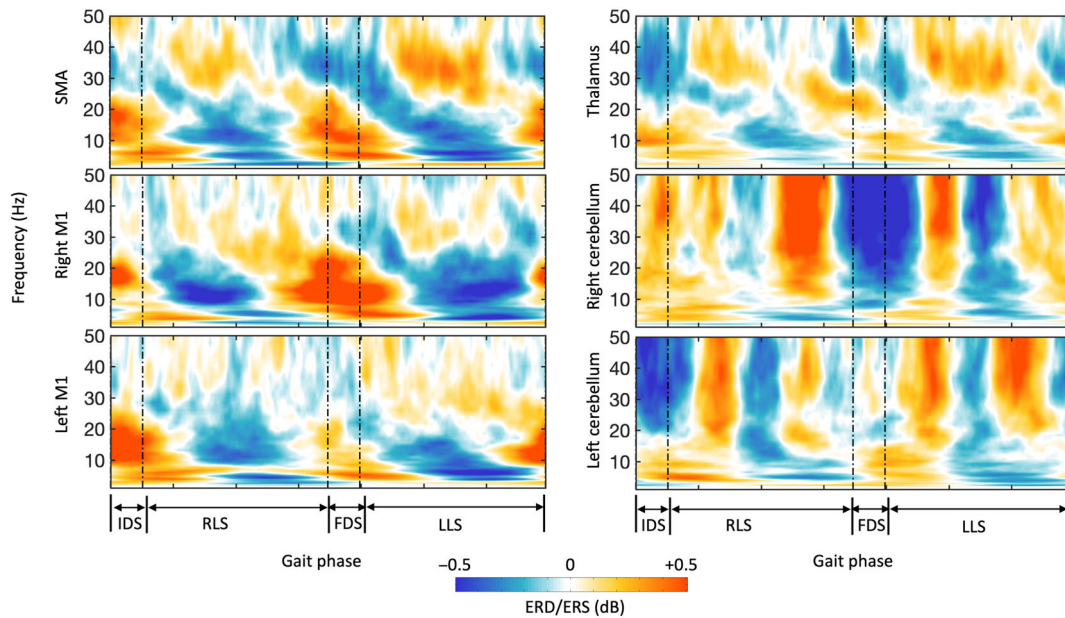
FIGURE 3 Event-related desynchronization/synchronization (ERD/ERS) in different cortical/subcortical regions. The four gait phases are indicated using dash lines on the time-frequency maps. The regions of interest (ROIs) are selected according to the following MNI coordinates: SMA [0, −8, 56], right M1 [34, −12, 68], left M1 [−34, −12, 68], thalamus [0, −18, 11], right cerebellum [27, −80, −38], and left cerebellum [−27, −80, −38]. SMA, supplementary motor area; M1, primary motor cortex; IDS, initial double support; RLS, right leg swing; FDS, final double support; LLS, left leg swing

FIGURE 4 Event-related desynchronization/synchronization (ERD/ERS) across frequencies and gait phases of different regions of interest (ROIs). The values represented in the matrices are the grand mean of the ERD/ERS values, for each frequency band and gait phase. α, alpha; β, beta; γ, gamma; SMA, supplementary motor area; M1, primary motor cortex; IDS, initial double support; RLS, right leg swing; FDS, final double support; LLS, left leg swing. *p_{FDR} <0.05; **p_{FDR} <0.01; ***p_{FDR} <.001
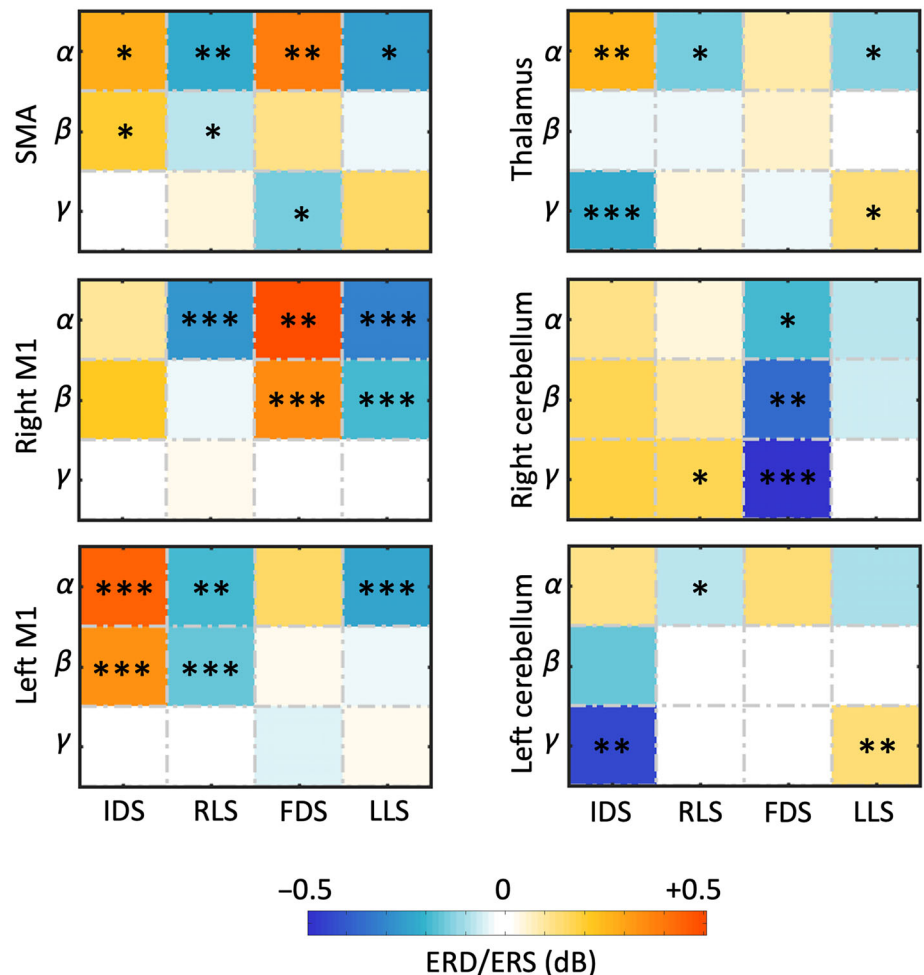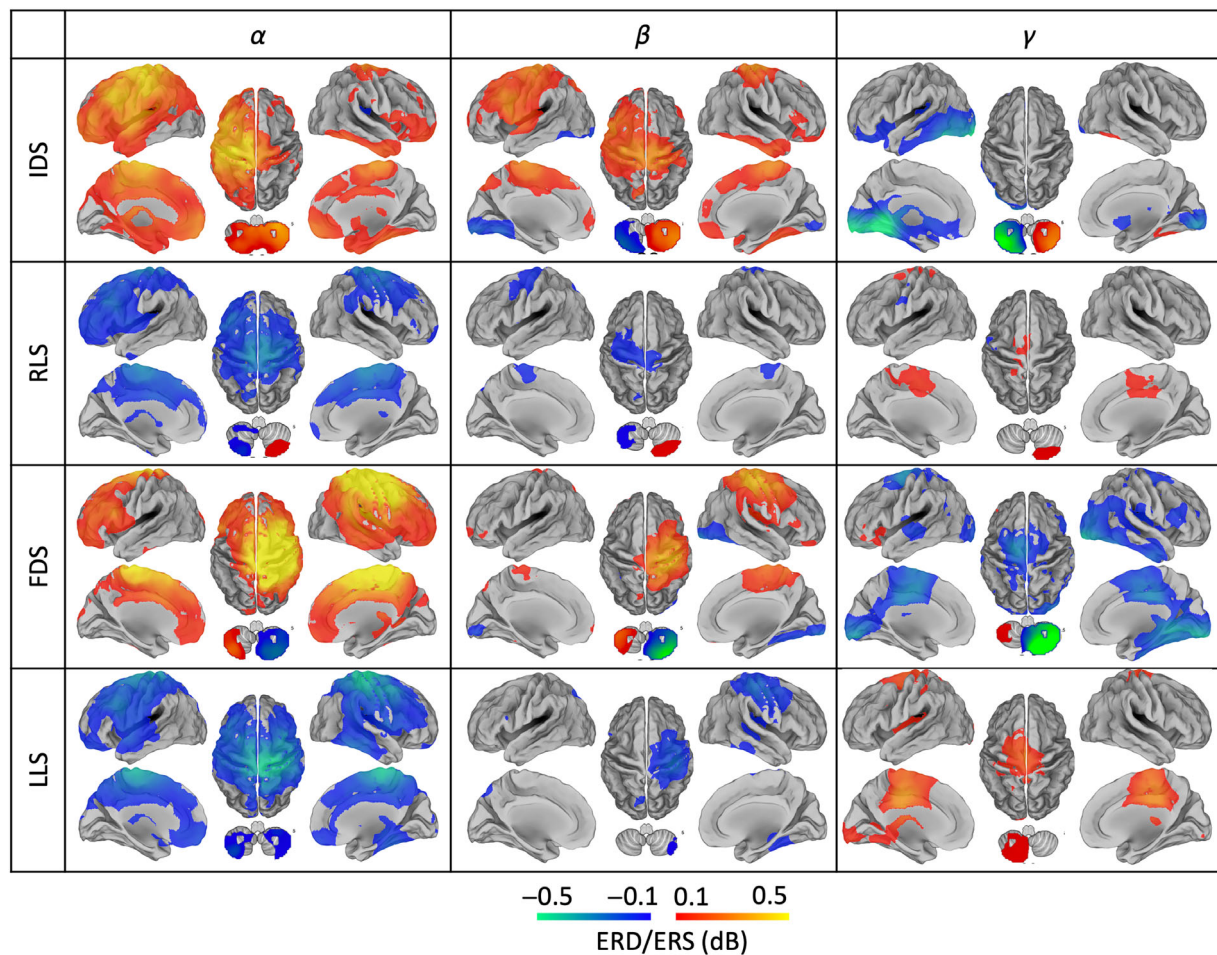
FIGURE 5 Event-related desynchronization/synchronization (ERD/ERS) maps for different frequency bands and gait phases. The values represented in each map are the grand mean of the ERS/ERD values, for specific frequency bands (α, β, and γ) and gait phases (IDS, RLS, FDS, and LLS). α, alpha; β, beta; γ, gamma; IDS, initial double support; RLS, right leg swing; FDS, final double support; LLS, left leg swing

for the attenuation of artifacts present in the EEG recordings, and relied on source-space EEG analyses capable of enhancing the spatial specificity of neural activity estimates. Our results showed that ERD/ERS modulations for alpha, beta, and gamma bands were strongest in the primary sensorimotor cortex (M1), but were also found in premotor cortex, thalamus and cerebellum. We observed a modulation of neural oscillations across gait phases in M1 and cerebellum, and an interaction between frequency band and gait phase in the premotor cortex and thalamus. Furthermore, an ERD/ERS lateralization effect was present in M1 for the alpha and beta bands, and in the cerebellum for the beta and gamma bands. We will more extensively discuss the methodological and neurophysiological aspects related to our work in the following sections.

4.1 | Methodological considerations

In previous EEG studies conducted in walking participants, the problem of movement and myogenic artifacts has been often overlooked. Specifically, artifact attenuation was either not performed (Gwin

et al., 2011; Nathan & Contreras-Vidal, 2016; Oliveira et al., 2017; Seeber et al., 2014; Seeber et al., 2015; Wagner et al., 2016), or single-step BSS was used to attenuate ocular, movement and myogenic artifacts that were mixed in the EEG recordings (An et al., 2019; Artoni et al., 2017; Bradford et al., 2016; Cortney Bradford et al., 2019; Gwin et al., 2011; Snyder et al., 2015), It has, however, been shown that, since BSS methods perform differently when separating the different kinds of artifacts (Barban et al., 2021; Fitzgibbon et al., 2007), the use of a single BSS method is suboptimal (Barban et al., 2021; Zhao et al., 2021). In the present study, we employed a novel multi-step BSS approach that attenuated different kinds of artifacts with artifact-specific filtering methods and classification parameters to minimize the impact of these artifacts in our mobile hdEEG data (Zhao et al., 2021).

Furthermore, a large number of movement-related EEG studies analyzed recordings in terms of scalp maps (Espenhahn et al., 2017; Pfurtscheller, 2001; Pfurtscheller & Lopes da Silva, 1999), or used BSS techniques to extract sensor-level components associated with neural activity (Artoni et al., 2017; Gwin et al., 2011; Snyder et al., 2015; Wagner et al., 2016). As such, they did not exploit the potential of

FIGURE 6 Dissociation of alpha, beta, and gamma oscillations across gait phases. The maps were generated by performing a voxel-wise two-way ANOVA with frequency and phase as factors on the event-related desynchronization/synchronization (ERD/ERS) maps of all the participants. The maps were thresholded at p < 0.01, with FDR correction
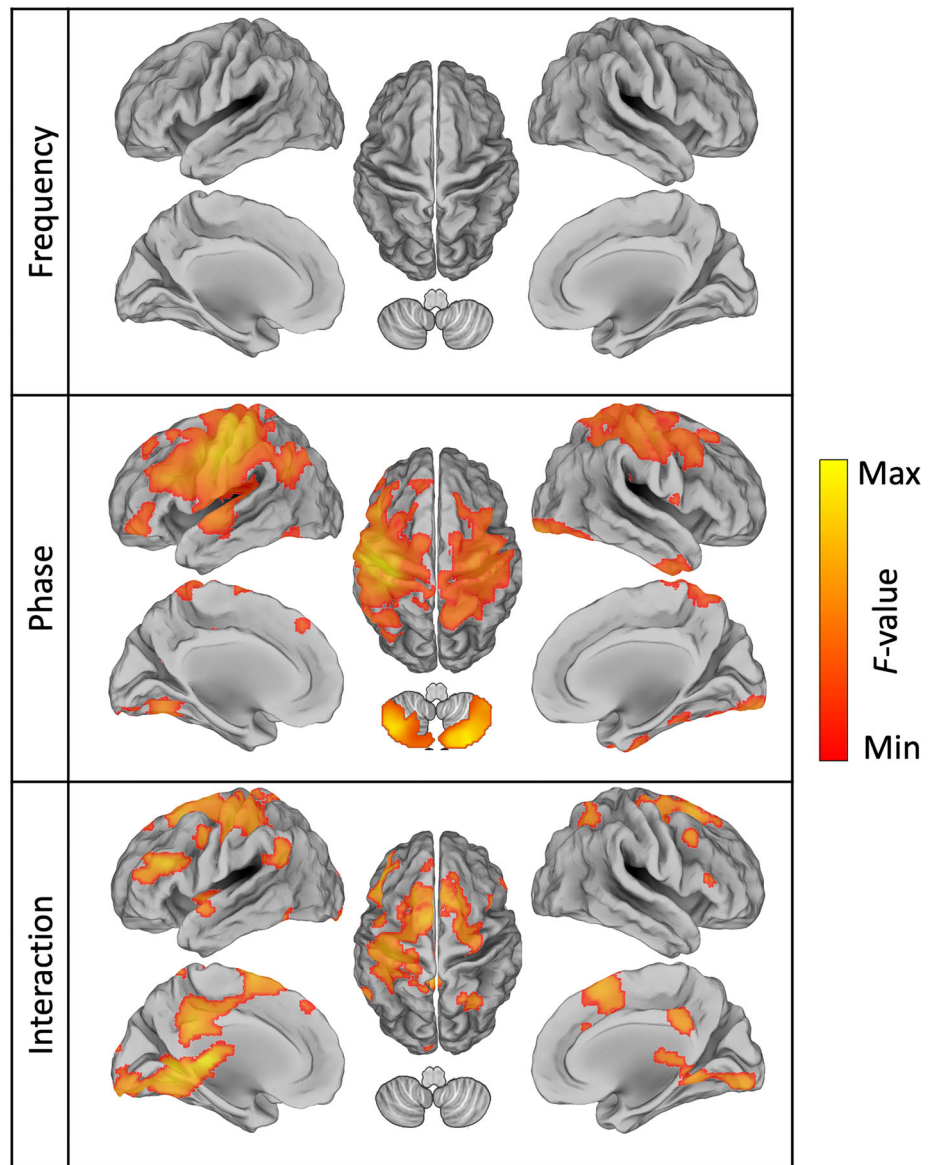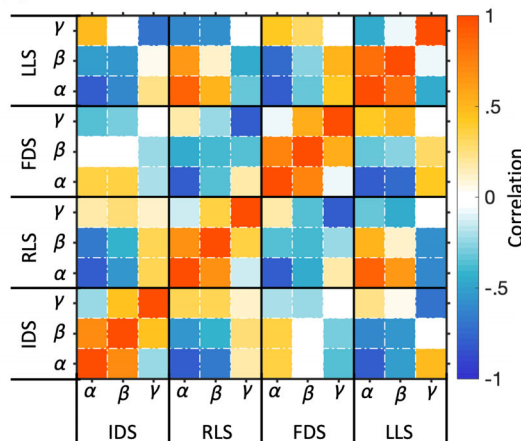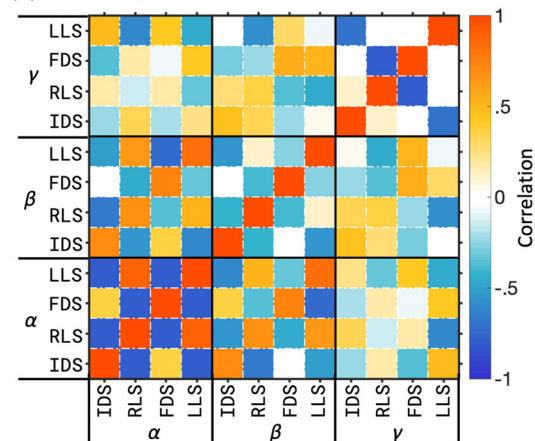
FIGURE 7 Similarities between event-related desynchronization/synchronization (ERD/ERS) maps across frequencies and gait phases, as measured by spatial correlation. The values of the correlation matrices are grouped (a) across gait phase and then frequency band, and (b) across frequency band and then gait phase. α, alpha; β, beta; γ, gamma; IDS, initial double support; RLS, right leg swing; FDS, final double support; LLS, left leg swing

EEG as a brain imaging technique (Michel & Murray, 2012). In a previous study, we showed that hdEEG, when combined with advanced techniques for head modeling and source localization, can be used to reveal movement-related neural dynamics in the human brain (Zhao et al., 2019). Specifically, we demonstrated that hand, foot and lip movements were characterized by specific neural signatures both in the frequency and space domains.

4.2 | Active neural sources during gait

We observed that gait-related neural modulations in alpha, beta, and gamma bands were most prominent in brain regions supporting sensory and motor functions (Figure 5). Consistent results were found both in our previous hdEEG study, in which participants performed leg movements while sitting (Zhao et al., 2019), and also in a number of magnetoencephalography studies on voluntary movement of body parts such as the finger, hand, and foot (Cheyne, 2013; Pfurtscheller, 2001; Pfurtscheller & Lopes da Silva, 1999; Sebastiani et al., 2014). Specifically, we observed that leg swing phases presented a sensorimotor ERD in the alpha and beta bands. Such an ERD during movement may directly indicate an increased recruitment of neurons in specific cortical regions for supporting the leg swing (Neuper et al., 2006; Pfurtscheller & Lopes da Silva, 1999), or may result from increased uncertainty estimates between sensory prediction and actual sensory input of the swinging leg (Tan et al., 2016). We also found that the alpha ERD during IDS and FDS was rather dorsal, whereas the alpha ERS during RLS and LLS was more ventral and lateralized. This finding suggests that the alpha oscillations may be related not only to sensorimotor processing, but also to other functions necessary for efficient motor control: for example, previous EEG studies documented a relationship between alpha oscillations and attention during performance of sensorimotor tasks (Babiloni et al., 2004; Deiber et al., 2012; Magosso et al., 2019; Neuper et al., 2006).

4.3 | Modulation of neural oscillations across frequency bands and gait phases

We also evaluated the voxel-wise differences across frequency bands and gait phases (Figure 6) and the global spatial similarity of ERD/ERS images (Figure 7). The ANOVA revealed significant modulation of brain oscillations across gait phases in bilateral sensorimotor cortex and cerebellum, as well as a significant interaction between phase and frequency in the premotor cortex and thalamus. The identification of these gait-related regions is consistent with fMRI and SPECT studies on leg movement (Christensen et al., 2000; Sahyoun et al., 2004) and imagery of walking (Bakker et al., 2008; Bakker, de Lange, et al., 2007; Jahn et al., 2004; Sacco et al., 2006). The spatial similarity analysis indicated significant positive correlations between adjacent bands in the same gait phase. This is also in line with a spatial similarity analysis on neighboring

frequency bands, conducted under controlled movement conditions (Zhao et al., 2019). A significant but less strong negative spatial correlation was observed between adjacent gait phases in the same frequency band, which might be associated with lateralized activations of left and right leg movements.

Neural activity during walking was examined in further detail for selected cortical and subcortical ROIs that have been previously reported to be related to gait performance (Bakker, Verstappen, et al., 2007). In cortical ROIs, we generally observed that alpha, beta, and gamma oscillations were modulated by the gait phase (Figure 3) in accordance with previous EEG studies (Seeber et al., 2014; Artoni et al., 2017). The modulations of alpha and beta bands in M1 showed clear lateralization effects during gait, similarly to what was previously observed with hdEEG for controlled foot movements (Zhao et al., 2019). Specifically, the beta ERD in the leg swing phases had a significantly stronger intensity in contralateral than ipsilateral M1 (Figure 4). This was not surprising, because beta ERD in one cerebral hemisphere is typically associated with the movement of the contralateral part of the body (Neuper et al., 2006; Pfurtscheller & Lopes da Silva, 1999; Stolk et al., 2019). The power fluctuations in the gamma band were more prominent in the SMA, and negatively correlated with the changes of alpha and beta power (Seeber et al., 2014, 2015). Dynamic modulations were also expected in subcortical regions such as the thalamus and cerebellum. The thalamus was found to be involved in the generation and monitoring of movement performance (Sommer, 2003). Previous self-paced movement studies reported alpha and beta ERD in the thalamus during motor preparation (Paradiso et al., 2004) and execution (Zhao et al., 2019). In our study, the ERD/ERS pattern in the thalamus was like the one in SMA, but with a stronger modulation in gamma than in alpha and beta bands (Figure 4). Electrophysiological signals produced by the cerebellum were previously reported to be detectable using EEG or MEG (Andersen et al., 2020), yet very little about these signals during gait is known. It should also be considered that the EEG signal measured close to the cerebellum is vulnerable to interference from neck muscle activations during walking (Richer et al., 2019). Although we used a validated approach to attenuate the impact of such artifacts in hdEEG signals (Zhao et al., 2021), the ERD/ERS results obtained for cerebellar regions should be interpreted cautiously.

4.4 | Limitations

We acknowledge that our current study has a number of limitations. First, our analysis was based on four gait phases due to the limitation of gait phase analysis using acceleration signals only. The use of a three dimensional infrared camera system (Pfister et al., 2014) or foot switches (Yan et al., 2021) could permit a detection of more gait phases (Silva & Stergiou, 2020), and may further improve the reliability of our source images in some brain regions such as the cerebellum. Secondly, our study only included a treadmill walking task; future investigation of overground free walking may reveal further information regarding the neural processes of gait control in circumstances

which require adaptation of stepping. Lastly, we examined gait-related neural dynamics in terms of band-limited power modulations; future analyses could also be conducted to evaluate frequency-dependent functional connectivity (Arce-McShane et al., 2016; Samogin et al., 2019, 2020) during gait performance.

5 | CONCLUSION

The findings presented in this study demonstrate that hdEEG recordings, in combination with appropriate artifact suppression and source-level analysis, allow the investigation of the event-related synchronization (ERS) and de-synchronization (ERD) dynamics across the gait cycle. Our future work will focus on the development of mobile hdEEG-based brain–body imaging (MoBI) platforms to enable overground walking investigations, with potential applications in the study of gait disorders.

CONFLICT OF INTEREST
The authors declare no conflict of interest.

AUTHOR CONTRIBUTIONS
Mingqi Zhao: Experimental design; methodology; data acquisition; data analysis; visualization; writing. **Gaia Bonassi**: Data acquisition; writing. **Jessica Samogin**: Methodology; writing. **Gaia Amaranta Taberna**: Methodology; writing. **Elisa Pelosin**: Conceptualization; data acquisition; writing. **Alice Nieuwboer**: Conceptualization; experimental design; writing. **Laura Avanzino**: Conceptualization; data acquisition; writing. **Dante Mantini**: Conceptualization; experimental design; methodology; visualization; writing.

DATA AVAILABILITY STATEMENT
The authors do not have permission to share raw data. The results produced in the present study are included in the article as well as the Supporting Information.

ORCID
Mingqi Zhao https://orcid.org/0000-0002-2804-9565
Gaia Bonassi https://orcid.org/0000-0003-2697-4113
Jessica Samogin https://orcid.org/0000-0002-9799-9003
Gaia Amaranta Taberna https://orcid.org/0000-0002-1989-6738
Elisa Pelosin https://orcid.org/0000-0002-9880-2241
Laura Avanzino https://orcid.org/0000-0001-6286-1509
Dante Mantini https://orcid.org/0000-0001-6485-5559

REFERENCES
Alamdari, A., & Krovi, V. N. (2017). Chapter 2—A review of computational musculoskeletal analysis of human lower extremities. In J. Ueda & Y. Kurita (Eds.), *Human modelling for bio-inspired robotics* (pp. 37–73). Academic Press.

Alexander, N. B. (1996). Gait disorders in older adults. *Journal of the American Geriatrics Society*, 44, 434–451.

An, W. W., Ting, K. H., Au, I. P. H., Zhang, J. H., Chan, Z. Y. S., Davis, I. S., So, W. K. Y., Chan, R. H. M., & Cheung, R. T. H. (2019). Neurophysiological correlates of gait retraining with real-time visual and auditory feedback. *IEEE Transactions on Neural Systems and Rehabilitation Engineering*, 27, 1341–1349.

Andersen, L. M., Jerbi, K., & Dalal, S. S. (2020). Can EEG and MEG detect signals from the human cerebellum? *NeuroImage*, 215, 116817.

Anderson, M., Adali, T., & Li, X.-L. (2011). Joint blind source separation with multivariate Gaussian model: Algorithms and performance analysis. *IEEE Transactions on Signal Processing*, 60, 1672–1683.

Arce-McShane, F. I., Ross, C. F., Takahashi, K., Sessle, B. J., & Hatsopoulos, N. G. (2016). Primary motor and sensory cortical areas communicate via spatiotemporally coordinated networks at multiple frequencies. *Proceedings of the National Academy of Sciences*, 113, 5083–5088.

Artoni, F., Fanciullacci, C., Bertolucci, F., Panarese, A., Makeig, S., Micera, S., & Chisari, C. (2017). Unidirectional brain to muscle connectivity reveals motor cortex control of leg muscles during stereotyped walking. *NeuroImage*, 159, 403–416.

Babiloni, C., Miniussi, C., Babiloni, F., Carducci, F., Cincotti, F., Del Percio, C., Sirello, G., Fracassi, C., Nobre, A. C., & Rossini, P. M. (2004). Sub-second "temporal attention" modulates alpha rhythms. A high-resolution EEG study. *Cognitive Brain Research*, 19, 259–268.

Baker, J. M. (2018). Gait disorders. *The American Journal of Medicine*, 131, 602–607.

Bakker, M., De Lange, F. P., Helmich, R. C., Scheeringa, R., Bloem, B. R., & Toni, I. (2008). Cerebral correlates of motor imagery of normal and precision gait. *NeuroImage*, 41, 998–1010.

Bakker, M., de Lange, F. P., Stevens, J. A., Toni, I., & Bloem, B. R. (2007). Motor imagery of gait: A quantitative approach. *Experimental Brain Research*, 179, 497–504.

Bakker, M., Verstappen, C. C. P., Bloem, B. R., & Toni, I. (2007). Recent advances in functional neuroimaging of gait. *Journal of Neural Transmission*, 114, 1323–1331.

Barban, F., Chiappalone, M., Bonassi, G., Mantini, D., & Semprini, M. (2021). Yet another artefact rejection study: An exploration of cleaning methods for biological and neuromodulatory noise. *Journal of Neural Engineering*, 18, 0460c0462.

Bradford, J. C., Lukos, J. R., & Ferris, D. P. (2016). Electrocortical activity distinguishes between uphill and level walking in humans. *Journal of Neurophysiology*, 115, 958–966.

Bulea, T. C., Kim, J., Damiano, D. L., Stanley, C. J., & Park, H.-S. (2015). Prefrontal, posterior parietal and sensorimotor network activity underlying speed control during walking. *Frontiers in Human Neuroscience*, 9, 247.

Castermans, T., Duvinage, M., Cheron, G., & Dutoit, T. (2014). About the cortical origin of the low-delta and high-gamma rhythms observed in EEG signals during treadmill walking. *Neuroscience Letters*, 561, 166–170.

Cheyne, D. O. (2013). MEG studies of sensorimotor rhythms: A review. *Experimental Neurology*, 245, 27–39.

Christensen, L. O. D., Johannsen, P., Sinkjær, T., Petersen, N., Pyndt, H. S., & Nielsen, J. B. (2000). Cerebral activation during bicycle movements in man. *Experimental Brain Research*, 135, 66–72.

Cortney Bradford, J., Lukos, J. R., Passaro, A., Ries, A., & Ferris, D. P. (2019). Effect of locomotor demands on cognitive processing. *Scientific Reports*, 9, 9234.

Deiber, M.-P., Sallard, E., Ludwig, C., Ghezzi, C., Barral, J., & Ibanez, V. (2012). EEG alpha activity reflects motor preparation rather than the mode of action selection. *Frontiers in Integrative Neuroscience, 6*, 59.

Espenhahn, S., de Berker, A. O., van Wijk, B. C. M., Rossiter, H. E., & Ward, N. S. (2017). Movement-related beta oscillations show high intra-individual reliability. *NeuroImage, 147*, 175–185.

Ferrari, M., & Quaresima, V. (2012). A brief review on the history of human functional near-infrared spectroscopy (fNIRS) development and fields of application. *NeuroImage, 63*, 921–935.

Fitzgibbon, S. P., Powers, D. M., Pope, K. J., & Clark, C. R. (2007). Removal of EEG noise and artifact using blind source separation. *Journal of Clinical Neurophysiology, 24*, 232–243.

Fukuyama, H., Ouchi, Y., Matsuzaki, S., Nagahama, Y., Yamauchi, H., Ogawa, M., Kimura, J., & Shibasaki, H. (1997). Brain functional activity during gait in normal subjects: A SPECT study. *Neuroscience Letters, 228*, 183–186.

Guarnieri, R., Marino, M., Barban, F., Ganzetti, M., & Mantini, D. (2018). Online EEG artifact removal for BCI applications by adaptive spatial filtering. *Journal of Neural Engineering, 15*, 056009.

Gwin, J. T., Gramann, K., Makeig, S., & Ferris, D. P. (2011). Electrocortical activity is coupled to gait cycle phase during treadmill walking. *NeuroImage, 54*, 1289–1296.

Hamacher, D., Herold, F., Wiegel, P., Hamacher, D., & Schega, L. (2015). Brain activity during walking: A systematic review. *Neuroscience and Biobehavioral Reviews, 57*, 310–327.

Haueisen, J., Ramon, C., Eiselt, M., Brauer, H., & Nowak, H. (1997). Influence of tissue resistivities on neuromagnetic fields and electric potentials studied with a finite element model of the head. *IEEE Transactions on Biomedical Engineering, 44*, 727–735.

Holdefer, R., Sadleir, R., & Russell, M. (2006). Predicted current densities in the brain during transcranial electrical stimulation. *Clinical Neurophysiology, 117*, 1388–1397.

Hyvarinen, A. (1999). Fast and robust fixed-point algorithms for independent component analysis. *IEEE Transactions on Neural Networks, 10*, 626–634.

Jahn, K., Deutschländer, A., Stephan, T., Strupp, M., Wiesmann, M., & Brandt, T. (2004). Brain activation patterns during imagined stance and locomotion in functional magnetic resonance imaging. *NeuroImage, 22*, 1722–1731.

Jasiewicz, J. M., Allum, J. H. J., Middleton, J. W., Barriskill, A., Condie, P., Purcell, B., & Li, R. C. T. (2006). Gait event detection using linear accelerometers or angular velocity transducers in able-bodied and spinal-cord injured individuals. *Gait & Posture, 24*, 502–509.

Kotiadis, D., Hermens, H. J., & Veltink, P. H. (2010). Inertial gait phase detection for control of a drop foot stimulator: Inertial sensing for gait phase detection. *Medical Engineering & Physics, 32*, 287–297.

Kurz, M. J., Wilson, T. W., & Arpin, D. J. (2012). Stride-time variability and sensorimotor cortical activation during walking. *NeuroImage, 59*, 1602–1607.

Laribi, M. A., & Zeghloul, S. (2020). Chapter 4—Human lower limb operation tracking via motion capture systems. In M. Ceccarelli & G. Carbone (Eds.), *Design and operation of human locomotion systems* (pp. 83–107). Academic Press.

Liu, Q., Balsters, J. H., Baechinger, M., van der Groen, O., Wenderoth, N., & Mantini, D. (2015). Estimating a neutral reference for electroencephalographic recordings: The importance of using a high-density montage and a realistic head model. *Journal of Neural Engineering, 12*, 056012.

Liu, Q., Farahibozorg, S., Porcaro, C., Wenderoth, N., & Mantini, D. (2017). Detecting large-scale networks in the human brain using high-density electroencephalography. *Human Brain Mapping, 38*, 4631–4643.

Liu, Q., Ganzetti, M., Wenderoth, N., & Mantini, D. (2018). Detecting large-scale brain networks using EEG: Impact of electrode density, head modeling and source localization. *Frontiers in Neuroinformatics, 12*, 4.

Magosso, E., Ricci, G., & Ursino, M. (2019). Modulation of brain alpha rhythm and heart rate variability by attention-related mechanisms. *AIMS Neuroscience, 6*, 1–24.

Mantini, D., Perrucci, M. G., Del Gratta, C., Romani, G. L., & Corbetta, M. (2007). Electrophysiological signatures of resting state networks in the human brain. *Proceedings of the National Academy of Sciences, 104*, 13170–13175.

Michel, C. M., & Murray, M. M. (2012). Towards the utilization of EEG as a brain imaging tool. *NeuroImage, 61*, 371–385.

Miyai, I., Tanabe, H. C., Sase, I., Eda, H., Oda, I., Konishi, I., Tsunazawa, Y., Suzuki, T., Yanagida, T., & Kubota, K. (2001). Cortical mapping of gait in humans: A near-infrared spectroscopic topography study. *NeuroImage, 14*, 1186–1192.

Nathan, K., & Contreras-Vidal, J. L. (2016). Negligible motion artifacts in scalp electroencephalography (EEG) during treadmill walking. *Frontiers in Human Neuroscience, 9*, 708.

Neuper, C., Wörtz, M., & Pfurtscheller, G. (2006). ERD/ERS patterns reflecting sensorimotor activation and deactivation. In C. Neuper & W. Klimesch (Eds.), *Progress in brain research* (pp. 211–222). Elsevier.

Oliveira, A. S., Schlink, B. R., Hairston, W. D., König, P., & Ferris, D. P. (2017). Restricted vision increases sensorimotor cortex involvement in human walking. *Journal of Neurophysiology, 118*, 1943–1951.

Paradiso, G., Cunic, D., Saint-Cyr, J. A., Hoque, T., Lozano, A. M., Lang, A. E., & Chen, R. (2004). Involvement of human thalamus in the preparation of self-paced movement. *Brain, 127*, 2717–2731.

Pascual-Marqui, R. D., Lehmann, D., Koukkou, M., Kochi, K., Anderer, P., Saletu, B., Tanaka, H., Hirata, K., John, E. R., & Prichep, L. (2011). Assessing interactions in the brain with exact low-resolution electromagnetic tomography. *Philosophical Transactions of the Royal Society A: Mathematical, Physical and Engineering Sciences, 369*, 3768–3784.

Pfister, A., West, A. M., Bronner, S., & Noah, J. A. (2014). Comparative abilities of Microsoft Kinect and Vicon 3D motion capture for gait analysis. *Journal of Medical Engineering & Technology, 38*, 274–280.

Pfurtscheller, G. (2001). Functional brain imaging based on ERD/ERS. *Vision Research, 41*, 1257–1260.

Pfurtscheller, G., & Lopes da Silva, F. H. (1999). Event-related EEG/MEG synchronization and desynchronization: Basic principles. *Clinical Neurophysiology, 110*, 1842–1857.

Richer, N., Downey, R.J., Nordin, A.D., Hairston, W.D., Ferris, D.P. (2019). Adding neck muscle activity to a head phantom device to validate mobile EEG muscle and motion artifact removal. 2019 9th International IEEE/EMBS Conference on Neural Engineering (NER), pp. 275–278.

Sacco, K., Cauda, F., Cerliani, L., Mate, D., Duca, S., & Geminiani, G. C. (2006). Motor imagery of walking following training in locomotor attention. The effect of 'the tango lesson'. *NeuroImage, 32*, 1441–1449.

Sahyoun, C., Floyer-Lea, A., Johansen-Berg, H., & Matthews, P. M. (2004). Towards an understanding of gait control: Brain activation during the anticipation, preparation and execution of foot movements. *NeuroImage, 21*, 568–575.

Samogin, J., Liu, Q., Marino, M., Wenderoth, N., & Mantini, D. (2019). Shared and connection-specific intrinsic interactions in the default mode network. *NeuroImage, 200*, 474–481.

Samogin, J., Marino, M., Porcaro, C., Wenderoth, N., Dupont, P., Swinnen, S. P., & Mantini, D. (2020). Frequency-dependent functional connectivity in resting state networks. *Human Brain Mapping, 41*, 5187–5198.

Schmeltzpfenning, T., & Brauner, T. (2013). 2 - foot biomechanics and gait. In A. Luximon (Ed.), *Handbook of footwear design and manufacture* (pp. 27–48). Woodhead Publishing.

Sebastiani, V., de Pasquale, F., Costantini, M., Mantini, D., Pizzella, V., Romani, G. L., & Della Penna, S. (2014). Being an agent or an observer: Different spectral dynamics revealed by MEG. *NeuroImage, 102*, 717–728.

Seeber, M., Scherer, R., Wagner, J., Solis-Escalante, T., & Müller-Putz, G. R. (2014). EEG beta suppression and low gamma modulation are different elements of human upright walking. *Frontiers in Human Neuroscience*, *8*, 485.

Seeber, M., Scherer, R., Wagner, J., Solis-Escalante, T., & Müller-Putz, G. R. (2015). High and low gamma EEG oscillations in central sensorimotor areas are conversely modulated during the human gait cycle. *NeuroImage*, *112*, 318–326.

Silva, L. M., & Stergiou, N. (2020). Chapter 7—The basics of gait analysis. In N. Stergiou (Ed.), *Biomechanics and gait analysis* (pp. 225–250). Academic Press.

Snyder, K. L., Kline, J. E., Huang, H. J., & Ferris, D. P. (2015). Independent component analysis of gait-related movement artifact recorded using EEG electrodes during treadmill walking. *Frontiers in Human Neuroscience*, *9*, 639.

Sommer, M. A. (2003). The role of thalamus in motor control. *Current Opinion in Neurobiology*, *13*, 663–670.

Stolk, A., Brinkman, L., Vansteensel, M. J., Aarnoutse, E., Leijten, F. S. S., Dijkerman, C. H., Knight, R. T., de Lange, F. P., & Toni, I. (2019). Electrocorticographic dissociation of alpha and beta rhythmic activity in the human sensorimotor system. *eLife*, *8*, e48065.

Storzer, L., Butz, M., Hirschmann, J., Abbasi, O., Gratkowski, M., Saupe, D., Schnitzler, A., & Dalal, S. S. (2016). Bicycling and walking are associated with different cortical oscillatory dynamics. *Frontiers in Human Neuroscience*, *10*, 61.

Studenski, S., Perera, S., Patel, K., Rosano, C., Faulkner, K., Inzitari, M., Brach, J., Chandler, J., Cawthon, P., Connor, E. B., Nevitt, M., Visser, M., Kritchevsky, S., Badinelli, S., Harris, T., Newman, A. B., Cauley, J., Ferrucci, L., & Guralnik, J. (2011). Gait speed and survival in older adults. *JAMA*, *305*, 50–58.

Sudarsky, L. (1990). Gait disorders in the elderly. *New England Journal of Medicine*, *322*, 1441–1446.

Suzuki, M., Miyai, I., Ono, T., & Kubota, K. (2008). Activities in the frontal cortex and gait performance are modulated by preparation—An fNIRS study. *NeuroImage*, *39*, 600–607.

Suzuki, M., Miyai, I., Ono, T., Oda, I., Konishi, I., Kochiyama, T., & Kubota, K. (2004). Prefrontal and premotor cortices are involved in adapting walking and running speed on the treadmill: An optical imaging study. *NeuroImage*, *23*, 1020–1026.

Taberna, G. A., Guarnieri, R., & Mantini, D. (2019). SPOT3D: Spatial positioning toolbox for head markers using 3D scans. *Scientific Reports*, *9*, 12813.

Taberna, G. A., Marino, M., Ganzetti, M., & Mantini, D. (2019). Spatial localization of EEG electrodes using 3D scanning. *Journal of Neural Engineering*, *16*, 026020.

Taberna, G. A., Samogin, J., & Mantini, D. (2021). Automated head tissue modelling based on structural magnetic resonance images for electroencephalographic source reconstruction. *Neuroinformatics*, *19*, 585–596.

Taberna, G. A., Samogin, J., Marino, M., & Mantini, D. (2021). Detection of resting-state functional connectivity from high-density electroencephalography data: Impact of head modeling strategies. *Brain Sciences*, *11*, 741.

Takakusaki, K. (2017). Functional neuroanatomy for posture and gait control. *Journal of Movement Disorders*, *10*, 1–17.

Tan, H., Wade, C., & Brown, P. (2016). Post-movement Beta activity in sensorimotor cortex indexes confidence in the estimations from internal models. *The Journal of Neuroscience*, *36*, 1516–1528.

Vorwerk, J., Oostenveld, R., Piastra, M. C., Magyari, L., & Wolters, C. H. (2018). The FieldTrip-SimBio pipeline for EEG forward solutions. *Biomedical Engineering Online*, *17*, 37.

Wagner, J., Makeig, S., Gola, M., Neuper, C., & Müller-Putz, G. (2016). Distinct β band oscillatory networks subserving motor and cognitive control during gait adaptation. *Journal of Neuroscience*, *36*, 2212–2226.

Yan, S.-H., Liu, Y.-C., Li, W., & Zhang, K. (2021). Gait phase detection by using a portable system and artificial neural network. *Medicine in Novel Technology and Devices*, *12*, 100092.

Zhao, M., Bonassi, G., Guarnieri, R., Pelosin, E., Nieuwboer, A., Avanzino, L., & Mantini, D. (2021). A multi-step blind source separation approach for the attenuation of artifacts in mobile high-density electroencephalography data. *Journal of Neural Engineering*, *18*, 066041.

Zhao, M., Marino, M., Samogin, J., Swinnen, S. P., & Mantini, D. (2019). Hand, foot and lip representations in primary sensorimotor cortex: A high-density electroencephalography study. *Scientific Reports*, *9*, 1–12.

SUPPORTING INFORMATION

Additional supporting information may be found in the online version of the article at the publisher's website.